TiO_2/Graphene Oxide and SiO_2 Nanocomposites Based on Poplar Wood Substrate under UV Irradiation and Negative Oxygen Ions Generation

Zhenxing Wang, Xiaoshuai Han, and Junwen Pu *

Indoor air quality is crucial to human health because poor air quality can easily lead to disease. To improve indoor air quality, it is essential to increase the concentration of negative oxygen ions in the air. Consequently, it is necessary to design a material that can generate negative oxygen ions indoors. In this study, a wood-based functional material was developed by anchoring TiO_2/graphene oxide (GO) and silica nanoparticles (SiO_2) onto wood. The results showed that the TiO_2/GO- and SiO_2-treated wood greatly enhanced the mechanical properties of the wood and increased the negative oxygen ion production to 1580 ions/cm^3 after 60 min of ultraviolet irradiation, which met the standard for fresh air. These treated wood materials could fulfil the pursuit by an individual for a healthy and environmentally friendly life, and represents a highly promising material in the application of indoor decoration materials.

Keywords: Negative oxygen ions; TiO_2; Graphene oxide; SiO_2; Wood

Contact information: Material Science and Technology, Beijing Forestry University, Beijing, China;
** Corresponding author: jwpu1964@163.com*

INTRODUCTION

Indoor air quality is closely related to quality of life, work efficiency, and physical health. According to the World Health Organization standards for fresh air, the negative ion concentration is an indicator of the air quality. Fresh air is defined as having a negative oxygen ion concentration that exceeds 1000 ions/cm^3 to 1500 ions/cm^3 (Gao *et al.* 2016). Negative oxygen ions, also known as air vitamins, can affect the quality of human life and the environment. Medical reports have shown that after inhaling negative oxygen ions for 30 min, the lungs can increase oxygen absorption by 20% and eliminate 14.5% of carbon dioxide, which substantially improves pulmonary function, blood circulation, and the mental state of a person (Tom *et al.* 1981; Sirota *et al.* 2006). Negative oxygen ions can also activate various enzymes in the body, promote metabolism, improve sleep quality, and enhance the resistance of the body to disease (Sirota *et al.* 2008). Negative ions also play a role in air purification because they can quickly neutralize secondhand smoke, odors, and specific volatile organic compounds (Daniels 2002). The concentration of negative oxygen ions in the air affects the lives of people at all times. Under natural conditions, the concentration of such ions may increase under a high pressure, strong ray effect, and after heavy rain. However, these methods are inconvenient for improving indoor conditions. For instance, although negative oxygen ions are produced under strong gamma ray irradiation, this method is detrimental to human health and has a low production rate (Sirota *et al.* 2006; Cosby *et al.* 1975; Walton *et al.* 2003). Consequently, a highly efficient photocatalyst was chosen in this study to provide energy of excitation and thereby cause oxygen molecules to ionize and produce negative oxygen ions.

In recent years, titanium dioxide (TiO_2) has become a popular and often investigated material in environmentally benign photocatalysis (Zeng *et al.* 2010; Zhang *et al.* 2013; Hou *et al.* 2015). However, the photocatalytic efficiency of pure TiO_2 is limited in practical applications because of the rapid recombination of light-induced electron charge carriers. Titanium dioxide generates electron-hole pairs upon irradiation with ultraviolet (UV) light and reacts with oxygen and water to form superoxide (O_2^-) and hydroxyl radicals (·OH); thus, the combination of oxide and TiO_2 can enhance the photocatalytic properties of a material (Shao *et al.* 2013; Cheng *et al.* 2014; Qiu *et al.* 2015).

Graphene oxide (GO) sheets possess good hydrophilic properties and are a two-dimensional carbon structure with rich oxygen-containing functional groups on the base surface plane. Thus, the deposition of metal oxides on GO sheets shows promise for improving the photocatalytic activity of TiO_2 (Jiang *et al.* 2011; Cong *et al.* 2013; Gao *et al.* 2014). Using a convenient sol-gel method, TiO_2 nanoparticles were deposited on GO sheets, and uneven patterns of TiO_2 formed on the surface of the GO flakes. However, the large specific surface area of GO, strong van der Waals interactions between the GO layers, and large-area π-π interactions caused heavy aggregation of the GO nanoplates in water. These conditions prevented abundant GO-containing oxygen from being exposed and weakened its practical application (Georgakilas *et al.* 2012; Wang *et al.* 2014; Yang *et al.* 2014). To overcome this defect, silica nanoparticles were added to the GO solution to expose potential oxygen-containing groups that accumulate in GO, thereby opening the aggregated GO layer to expose more oxygen-containing groups (Yang *et al.* 2015). The addition of silica greatly increased the contact between the TiO_2 and GO, which effectively reduced the recombination of electrons and holes during the photocatalytic process, while increasing the production of negative oxygen ions (O_2^-).

As a fast-growing material with a short growth cycle, poplar wood has been used widely in the fields of architecture and furniture because of its beautiful appearance, light weight, thermal expansion, and renewability. However, it possesses several drawbacks, such as a poor mechanical stability, dimensional stability, and corrosion resistance, all of which greatly limit its potential applications (Gao *et al.* 2015b). Therefore, it is necessary to address the weaknesses of poplar to realize functional improvements. Conventional wood modification methods are generally complex, difficult to manipulate, costly, and likely to cause environmental pollution (Shi *et al.* 1996; Byrappa and Adschiri 2007; Gao *et al.* 2015a; Yao *et al.* 2016). Hence, there is strong interesting in finding a simple, low-cost, easily processed, and environmentally benign approach to the modification of wood and its utilization in composites.

Based on the above considerations, this paper considered the anchoring of TiO_2/GO and silica nanoparticles (SiO_2) on a wood substrate. A simple and effective strategy was proposed to transform the original wood into a high-performance structural material with better dimensional stability, mechanical properties, corrosion resistance, and negative oxygen ion generation under UV irradiation.

EXPERIMENTAL

Materials

All of the reagents were purchased from Ke Bai Ao Co. (Beijing, China). The reagents used were a GO solution (0.25% w/w), neutral silica sol (SiO_2; 30% ± 1%; pH:

7.5 to 8.5; particle size: 10 nm to 20 nm), and TiO_2 (AS-9306). Deionized water was used throughout the study. Poplar wood was obtained from the northern base of Beijing Forestry University; the trees were approximately 4 years to 5 years old. The wood samples were oven-dried (24 h and 103 °C ± 2 °C) to a constant weight after being ultrasonically rinsed in deionized water for 30 min.

Methods

Synthesis of the TiO_2/GO and SiO_2 nanocomposite modifier

The TiO_2/GO modifier were prepared *via* a simple modified sol-gel method at room temperature (25 °C). The GO solution 1% w/w (based on the mass of modifier) and neutral silica sol 15% w/w were suspended in deionized water 69% w/w under continuous stirring for 1 h. Then, the photocatalyst 15% w/w was added to the mixed solution under continuous stirring for 5 h. Finally, the modifier was obtained.

Vacuum pressure impregnation

The poplar wood logs were peeled and sawn into blocks measuring approximately 300 mm (longitudinal) × 200 mm (tangential) × 30 mm (radial). First, the wood samples were placed in an impregnation tank and subjected to a vacuum treatment under reduced pressure at -0.08 MPa to 0.1 MPa for 2 h. Then, the modifier was injected until the impregnation tank was filled with the solution. Subsequently, a pressurized treatment was performed at a pressure of 0.6 MPa to 0.8 MPa for 2 h. Finally, the wood loaded with TiO_2/GO and SiO_2 was removed and air-dried for 3 d to 4 d at room temperature (20 °C) to obtain TiO_2/GO- and SiO_2-treated wood.

Mechanical properties

The density, bending strength, and compressive strength parallel to the grain of the original and treated wood were measured according to the Chinese standards GB/T 1933–2009, GB/T 1936.1–2009, and GB/T 1935–2009, respectively. The surface hardness was tested using a TH210 hardness tester (Beijing TIME High Technology Ltd., Beijing, China) and the shore D hardness according to ASTM D2240 standard (Gooch 2011). Furthermore, the dimensions of the samples tested for the bending strength and compression perpendicular to the grain were 300 mm × 20 mm × 20 mm and 30 mm × 20 mm × 20 mm, respectively. The required size for the other test samples was 20 mm × 20 mm × 20 mm. To ensure rigorous experimental data, the measured values for each test were recorded based on the average of 10 samples.

Weight percent gain

The weight percent gain (WPG) after vacuum pressure impregnation was calculated according to Eq. 1. The measurements were repeated using 10 samples,

$$WPG\ (\%) = 100(W_i - W_0) / W_0 \quad (1)$$

where W_i is the oven-dry weight of the wood samples after impregnation (g), and W_0 is the oven-dried weight of the original wood samples (g).

Water uptake

Water absorption tests on the original and modified wood were performed at room temperature (20 °C). Each sample was soaked in water for 12 d with the weight measured at various intervals. Before each measurement, a clean cloth was used to remove excess

water from the sample surface. Each set of tests recorded data for 10 samples and the average value was reported. The water uptake (%) was calculated with Eq. 2,

$$W\,(\%) = 100(M_i - M_0) / M_0 \quad (2)$$

where M_i is the final mass (g), and M_0 is the original mass (g).

X-ray diffraction

X-ray diffraction (XRD) was used to study the crystal structure and degree of crystallinity of the TiO_2/GO- and SiO_2-treated and original wood. The XRD analysis was performed at room temperature at a scanning rate of 2°/min using an XRD 6000 X-ray diffractometer (Shimadzu, Kyoto, Japan) (40 kV and 30 mA). The relative crystallinity was obtained using the ratio of the sample crystallinity to that of a standard amorphous material. The degree of crystallinity (*Cr*) was calculated according to Eq. 3,

$$Cr\,(\%) = 100F_c / (F_a + F_c) \quad (3)$$

where F_c is the intensity of the crystalline region, and F_a is the corresponding intensity in the amorphous region.

Fourier transform infrared spectroscopy

Fourier transform infrared (FTIR) spectra were recorded using a Tensor 27 (Bruker, Karlsruhe, Germany) over a scanning range of 4000 cm^{-1} to 400 cm^{-1} with a resolution of 2 cm^{-1} for 32 scans. The original and treated wood samples were ground into a 120-mesh particle size and mixed with potassium bromide pellets at a 1:80 ratio.

Field emission scanning electron microscopy

The morphology of the original and treated wood was determined using field emission scanning electron microscopy (FESEM) (SU-8020, Hitachi, Tokyo, Japan). The required working distance was 20 nm with a lighting current of 0.7 Na and acceleration voltage of 1 kV. The original and treated wood samples were cut into small wooden bars that measured 10 mm × 1.5 mm × 1.5 mm.

Negative oxygen ion production tests under ultraviolet irradiation

The negative oxygen ion concentration was determined using an AIC1000 air anion counter (Shuangxu, Shanghai, China). The samples were placed in an obturator measuring 500 mm (length) × 300 mm (width) × 300 mm (height). The samples underwent UV irradiation at a wavelength of 400 nm during the experiment. The air anion counter was rezeroed before starting the test at a resolution ratio of 10 ions/cm^3 at 5-min intervals. Each set of negative oxygen ion production under UV irradiation lasted for 60 min, and the negative oxygen ion concentration was measured every 5 min.

RESULTS AND DISCUSSION

Functional Modifier

The synthetic modification reagents are shown in Fig. 1. Figure 1 shows that the solution without SiO_2 contained a large number of visible flocculation particles caused by large-area π-π interactions and strong van der Waals interactions between the GO layers (Yang *et al.* 2015). This modifier had difficulty meeting the wood modification

requirements; the flocculation of GO particles caused a notable reduction in the binding to TiO_2, which is inefficient for the production of negative oxygen ions (Ali *et al.* 2017). However, the flocculation particles disappeared when the silica was added to the solution (Fig. 1). The functional group of GO nanosheets would be exposed owing to the addition of SiO_2, which could reduce the restacking of the GO nanosheets (Yang *et al.* 2014; Liu *et al.* 2013). Thus the expected requirements for the modifier were met.

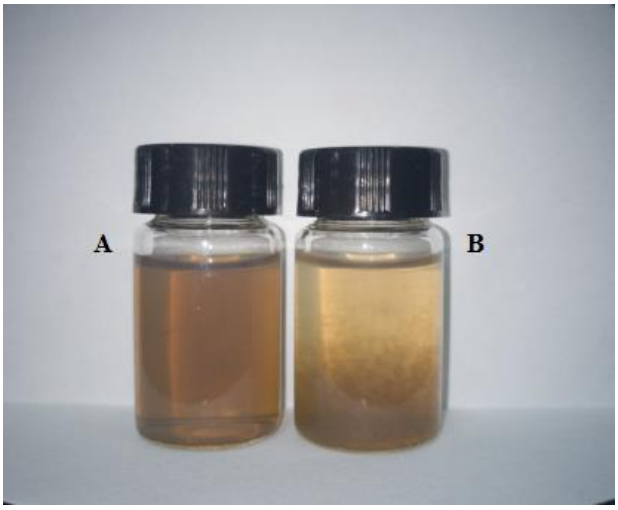

Fig. 1. Modifier: (A) TiO_2/GO with SiO_2; and (B) TiO_2/GO without SiO_2

Mechanical Properties

The density and mechanical properties of the original and TiO_2/GO- and SiO_2-treated wood samples (data averaged from 10 specimens) are shown in Table 1. The air-dried density of the TiO_2/GO- and SiO_2-treated wood increased by 21.6% compared with that of the original wood, from 0.37 g/cm^3 to 0.45 g/cm^3; the oven-dried density increased by 42.5%. The surface hardness of the treated wood was 21.4% greater than that of the original wood. The bending strength and compressive strength parallel to the grain of the treated wood were remarkably superior to those of the original wood. The treated wood demonstrated the highest bending strength of 106.3 MPa, which was 1.5 times higher than that of the untreated natural wood.

Table 1. Mechanical Properties of the Original and Treated Wood Samples

Property	Original Wood	Treated	Improvement
Air-dried Density (g/cm^3)	0.37 ± 0.05	0.45 ± 0.06	21.62%
Density (g/cm^3)	0.40 ± 0.08	0.57 ± 0.03	42.50%
Compressive Strength Parallel to the Grain (MPa)	42.43 ± 2.64	74.56 ± 4.33	75.72%
Bending Strength (MPa)	69.38 ± 9.78	106.32 ± 6.43	53.24%
Hardness (shore D)	45.80 ± 2.47	55.58 ± 3.42	21.35%
WPG (%)	-	28.50 ± 1.63	-

The compressive strength parallel to the grain increased by 75.7%. This data indicated that the mechanical properties of the treated wood were enhanced by the reaction between the modifier and wood cells. Compared with the mechanical properties of the original wood, the treated wood exhibit more obvious improvement. The test results were also in line with the expectations that excellent modifiers should exhibit better mechanical properties. Each set of tests had the same external conditions.

Water Uptake

The results of water absorption for the original and treated wood at room temperature are shown in Fig. 2. The water resistance of the treated wood was significantly improved compared to the original wood. The water absorption of the treated wood was less than that of the original wood in the 12-d test. Both sets of test curves increased substantially after approximately 1 d and then flattened after 8 d, which indicated that the present synthesis strategy successfully achieved combination of the TiO_2/GO and SiO_2 nanocomposites with the wood water-absorbing groups. This reduced the number of hydroxyl groups in the wood. The addition of SiO_2 effectively resolved the issue of substantial aggregation of the GO solution, and SiO_2 produced by the drying and solidification of silica sol blocked the holes in the surface of the wood; thus, the opportunity to combine wood with water molecules was reduced (Rahman *et al.* 2010).

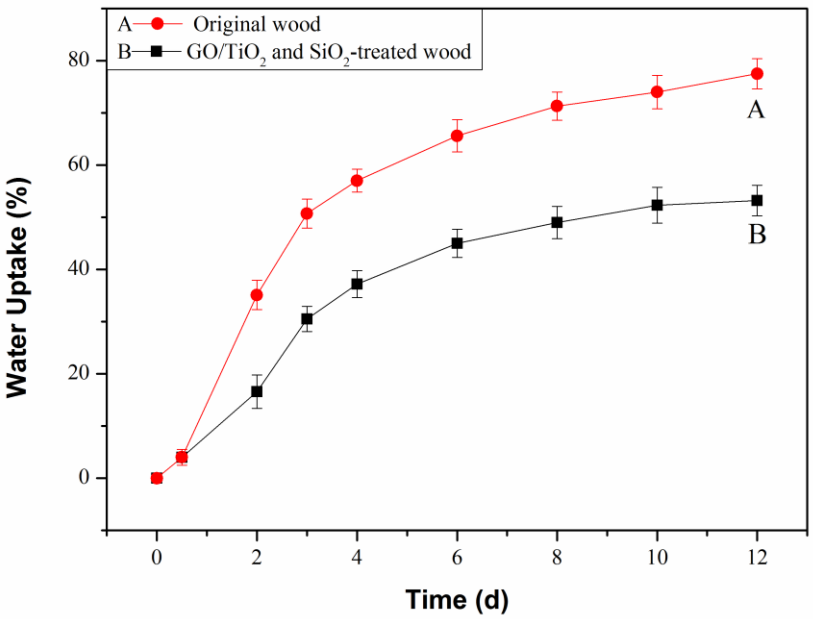

Fig. 2. Water uptake of the (A) original and (B)TiO_2/GO and SiO_2-treated wood

XRD Analysis

Figure 3 shows the crystallinity of the original and TiO_2/GO- and SiO_2-treated wood that was determined using XRD analysis. The original wood showed a maximum intensity at a 2θ of 16.1° (cellulose crystal diffraction, 101), and the curve extended to a minimum of 18°, which is a region characteristic of amorphous cellulose. The most remarkable diffraction peak of cellulose (002) appeared near 22.5°, and a small diffraction peak (040) appeared around 35° (Cave 1997). Based on these findings, the crystallinity of

the original wood was 22.4%, whereas that of the treated wood was 21.3%. Compared with the original wood, the change in the position of the treated wood peaks was small, which suggested that the modified solvent did not destroy the basic structure of the wood during the impregnation process. The reason for the slight decrease in the crystallinity was speculated to have been because the nanoparticles in the reaction solvent increased the spatial size of the amorphous region, which resulted in the expansion of the amorphous region (Fu *et al.* 2006).

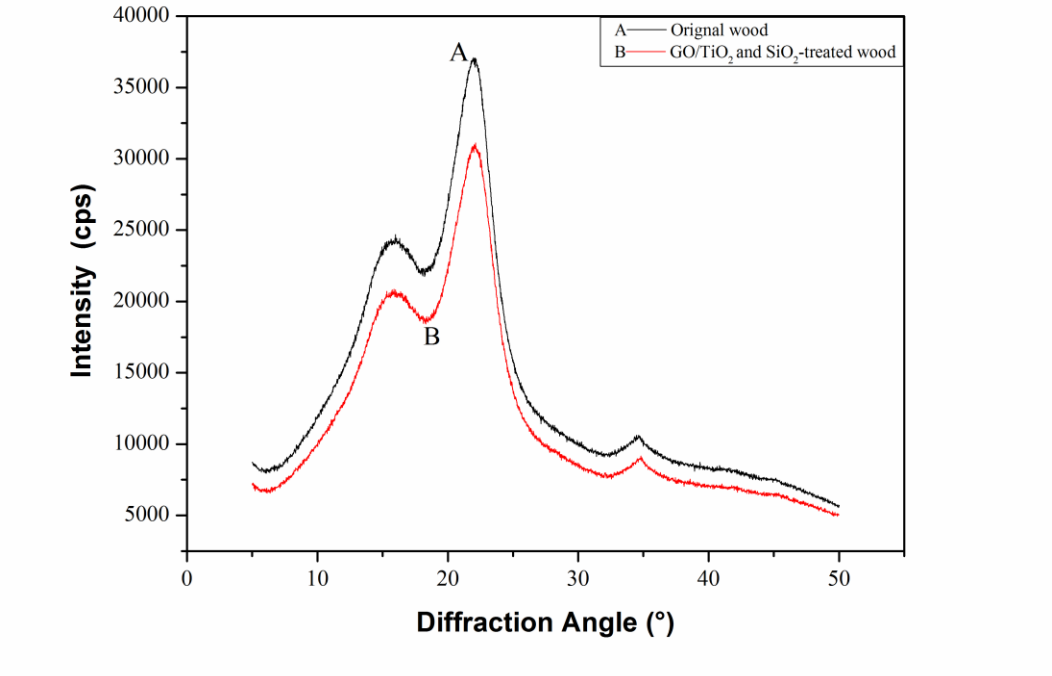

Fig. 3. XRD patterns of the (A) original and (B) TiO_2/GO- and SiO_2-treated wood

FTIR Analysis

The FTIR spectra of the original and treated wood samples are illustrated in Fig. 4. The original wood bands at 1050 cm^{-1} and 3400 cm^{-1} indicated that -OH stretching and vibration of various polysaccharides were pronounced (Horikawa *et al.* 2006; Devi and Maji 2012). Peaks appeared around 1250 cm^{-1} (Si-O-C), 812 cm^{-1} (Si-O), and 705 cm^{-1} (Si-O-Si), which were attributed to the presence of silica (Gwon *et al.* 2010).

Field Emission Scanning Electron Microscopy Analysis

The FESEM images in Fig. 5 show the microstructural features of the TiO_2/GO- and SiO_2-treated wood. The original wood surface had unevenly sized holes, which indicated that the poplar wood was a heterogeneous and porous material before being modified. After the vacuum-pressure impregnation, the wood surface was covered by TiO_2/GO and SiO_2 microparticles (Fig. 5B). The holes of the modified wood were filled with modifier particles. These close-knit accumulated modifiers could play a key role in protecting the wood from various forms of damage in addition to enhancing the structural strength of the wood and reducing the water absorption (Zou *et al.* 2008). The SEM studies showed that the modifier had been successfully impregnated into the cell cavity/wall of wood, thus contributing to the above obviously improved mechanical properties and water resistance (Tan and Cheetham 2011).

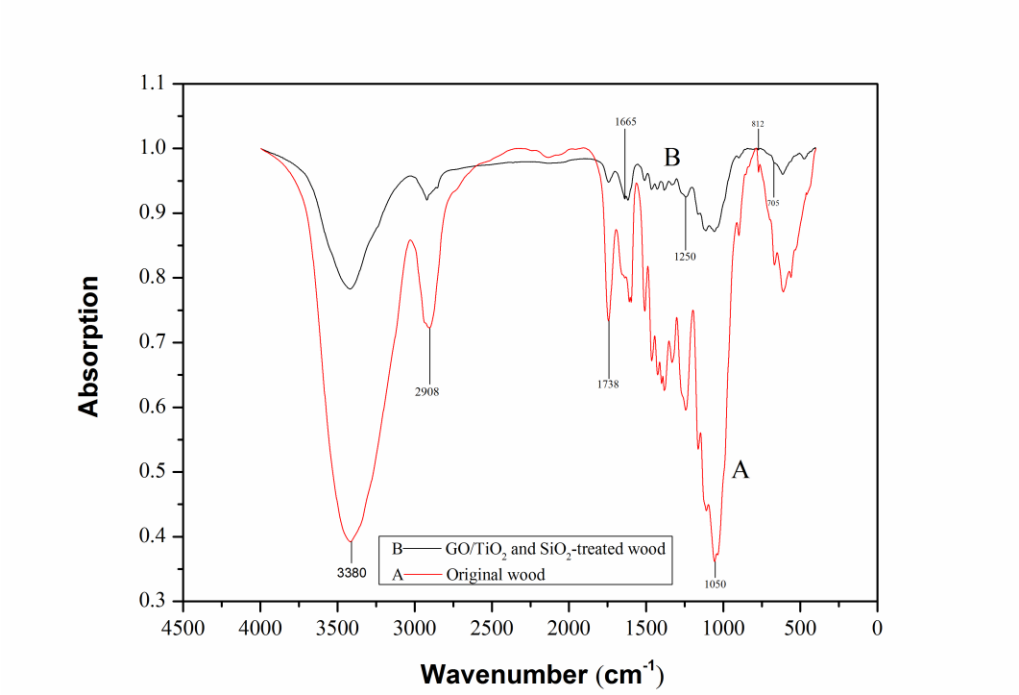

Fig. 4. FTIR spectra of the (A) original and (B) TiO_2/GO- and SiO_2-treated wood

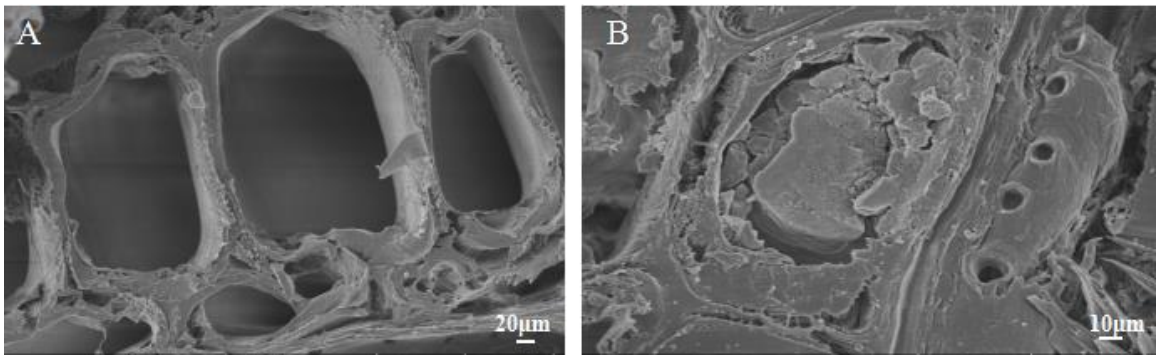

Fig. 5. FESEM images of the (A) original and (B) TiO_2/GO- and SiO_2-treated wood

Negative Oxygen Ion Concentration

The results from negative oxygen ion concentration-measurements are shown in Fig. 6. The initial negative oxygen ion concentration in the obturator, where the sample was exposed to UV light, was 0.0 ions/cm^3. The absence of irradiation without the sample group demonstrated that the internal environment of the obturator had no negative effects on the experimental results. Figure 6 illustrates that the negative oxygen ion concentration produced by the TiO_2/GO- and SiO_2-treated wood increased substantially and was larger than that of the original and TiO_2/GO-treated wood after 60 min of irradiation. The negative oxygen ion concentration of the TiO_2/GO-treated wood was slightly higher than that of the original wood during the entire UV irradiation process. After 45 min of irradiation, the negative oxygen ion concentrations in the three sample groups decreased slightly, but that of the TiO_2/GO- and SiO_2-treated wood was still higher than that of the TiO_2/GO-treated and original wood. After 1 h of irradiation, the concentrations of the TiO_2/GO- and SiO_2-treated, TiO_2/GO-treated, and original wood were 1580 ions/cm^3, 920 ions/cm^3, and 400

ions/cm^3, respectively. After 60 min of irradiation, only the TiO_2/GO- and SiO_2-treated wood had a concentration greater than 1000 ions/cm^3 and was able to meet the standard for fresh air (Zhong *et al.* 1998). The results also indicated that the addition of GO and SiO_2 effectively enhanced the production of negative oxygen ions. To further confirm the efficiency of the negative oxygen ions generated by the photocatalyst under UV irradiation, the time from 60 min to 120 min in Fig. 6 indicated that the sample generated a negative oxygen ion content when the UV light was off. The overall trend of generating negative oxygen ions by the three sample groups was gradually reduced. After 60 min without irradiation, the concentrations of the TiO_2/GO- and SiO_2-treated, TiO_2/GO-treated, and original wood were 1260 ions/cm^3, 550 ions/cm^3, and 80 ions/cm^3, respectively. The negative oxygen ion concentration of the TiO_2/GO- and SiO_2-treated wood still met the standard for fresh air.

Then, the UV light was turned on again to determine the durability and practicality of the TiO_2/GO- and SiO_2-treated wood. As depicted from 120 min to 180 min in Fig. 6, the concentrations of the TiO_2/GO- and SiO_2-treated, TiO_2/GO-treated, and original wood after 60 min of irradiation were 1560 ions/cm^3, 880 ions/cm^3, and 390 ions/cm^3, respectively. The performance stability of the TiO_2/GO- and SiO_2-treated wood was still better than that of the TiO_2/GO-treated and original wood, and the negative oxygen ion concentration released by the TiO_2/GO- and SiO_2-treated wood continued to meet the standard for fresh air.

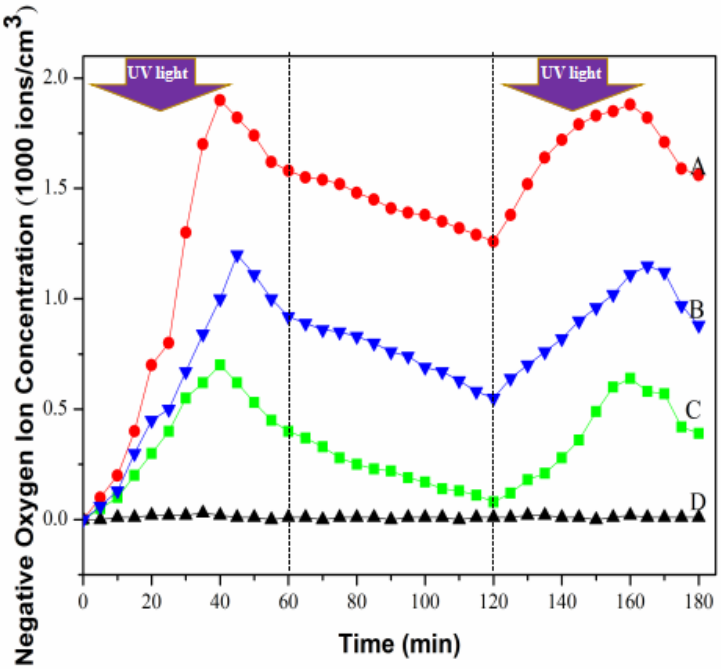

Fig. 6. Negative oxygen ion concentrations in the obturator with the samples surface under UV irradiation: (A) TiO_2/GO- and SiO_2-treated wood, (B) TiO_2/GO-treated wood, (C) original wood, and (D) sample without irradiation

Photocatalysis Mechanism

When TiO_2/GO composites were irradiated by UV light with energy equal to or greater than the energy band, the GO acted as an electron acceptor in the TiO_2/GO combination and reduced the charge recombination. The charges e^- and h^+ were generated

in the TiO_2/GO composites, which caused excited electrons in the conduction band of the TiO_2 to be transferred into the GO (Zhou *et al.* 2011). This left a positive charge in the valence band of the TiO_2. Subsequently, the h^+ reacted with H_2O or hydroxide ions (OH^-) to generate hydroxyl radicals (·OH), and the e^- reacted with O_2 to generate negative oxygen ions (O_2^-) (Khalid *et al.* 2013; Posa *et al.* 2016). The negative oxygen ion production process under UV irradiation (Fig. 7) is expressed with Eqs. 4 through 7:

$$TiO_2/GO + hv \rightarrow TiO_2(h^+) + GO(e^-) \quad (4)$$

$$h^+ + H_2O \rightarrow \cdot OH + H^+ \quad (5)$$

$$h^+ + OH^- \rightarrow \cdot OH \quad (6)$$

$$GO(e^-) + O_2 \rightarrow GO + O_2^- \quad (7)$$

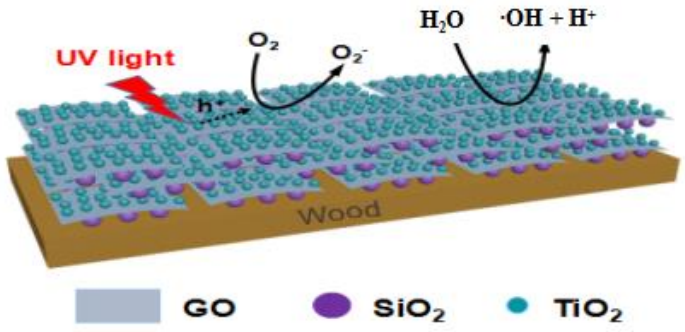

Fig. 7. Possible scheme for negative oxygen ion production from the TiO_2/GO- and SiO_2-treated wood under UV irradiation

CONCLUSIONS

1. The mechanical properties of the TiO_2/GO- and SiO_2-treated wood, including the density, bending strength, compressive strength parallel to the wood grain, and hardness, were remarkably enhanced compared with that of the original wood. After being modified with TiO_2/GO and SiO_2, the modified solvent was immersed in the wood pores. The modifier reacted with the hydroxyls and other free radicals in the cell and generated hydrogen bonds, while blocking the pores of the wood surface, thereby reducing the likelihood of contact between moisture-absorbing groups in the wood and water molecules.
2. Compared with the original wood, the treated wood released sufficient negative oxygen ions to improve the air quality and meet the standard for fresh air. The presence of negative oxygen ions is beneficial to the physical and mental health of people.
3. Regarding the overall experimental procedure of wood processing, this method is simple, and it utilizes environmentally friendly materials, all of which align with the social requirements for sustainable development.

ACKNOWLEDGEMENTS

The authors are grateful for the financial support of a special fund from the Beijing Common Construction Project and Beijing Forestry University (Grant No. 2016HXKFCLXY001).

REFERENCES CITED

Ali, I., Park, K., Kim, S. R., and Kim, J. O. (2017). "Electrochemical anodization of graphite oxide-TiO_2 nanotube composite for enhanced visible light photocatalytic activity," *Environmental Science & Pollution Research*, 1-10. DOI: 10.1007/s11356-017-8571-y

Byrappa, K., and Adschiri, T. (2007). "Hydrothermal technology for nanotechnology," *Prog. Cryst. Growth Ch.* 53(2), 117-166. DOI: 10.1016/j.pcrysgrow.2007.04.001

Cave, I. D. (1997). "Theory of X-ray measurement of microfibril angle in wood," *Wood Sci. Technol.* 31(3), 143-152. DOI: 10.1007/bf00705881

Cheng, C., Amini, A., Zhu, C., Xu, Z., Song, H., and Wang, N. (2014). "Enhanced photocatalytic performance of TiO_2-ZnO hybrid nanostructures," *Sci. Rep.-UK* 4. DOI: 10.1038/srep04181

Cong, Y., Long, M., Cui, Z., Li, X., Dong, Z., Yuan, G., and Zhang, J. (2013). "Anchoring a uniform TiO_2 layer on graphene oxide sheets as an efficient visible light photocatalyst," *Appl. Surf. Sci.* 282, 400-407. DOI: 10.1016/j.apsusc.2013.05.143

Cosby, P. C., Bennett, R. A., Peterson, J. R., and Moseley, J. T. (1975). "Photodissociation and photodetachment of molecular negative ions. II. Ions formed in oxygen," *J. Chem. Phys.* 63(4), 1612-1620. DOI: 10.1063/1.431487

Daniels, S. L. (2002). "On the ionization of air for removal of noxious effluvia (Air ionization of indoor environments for control of volatile and particulate contaminants with nonthermal plasmas generated by dielectric-barrier discharge)," *IEEE T. Plasma Sci*. 30(4), 1471-1481. DOI: 10.1109/TPS.2002.804211

Devi, R. R., and Maji, T. K. (2012). "Chemical modification of simul wood with styrene-acrylonitrile copolymer and organically modified nanoclay," *Wood Sci. Technol.* 46(1-3), 299-315. DOI: 10.1007/s00226-011-0406-2

Fu, Y., Zhao, G., and Chun, S. (2006). "Microstructure and physical properties of silicon dioxide/wood composite," *Acta Materiae Compositae Sinica* 23(4), 52-59.

Gao, P., Li, A., Sun, D. D., and Ng, W. J. (2014). "Effects of various TiO_2 nanostructures and graphene oxide on photocatalytic activity of TiO_2," *J. Hazard. Mater.* 279, 96-104. DOI: 10.1016/j.jhazmat.2014.06.061

Gao, L., Gan, W., Xiao, S., Zhan, X., and Li, J. (2015a). "Enhancement of photo-catalytic degradation of formaldehyde through loading anatase TiO_2 and silver nanoparticle films on wood substrates," *RSC Adv.* 5(65), 52985-52992. DOI: 10.1039/C5RA06390F

Gao, L., Xiao, S., Gan, W., Zhan, X., and Li, J. (2015b). "Durable superamphiphobic wood surfaces from Cu_2O film modified with fluorinated alkyl silane," *RSC Adv.* 5(119), 98203-98208. DOI: 10.1039/c5ra19433d

Gao, L., Qiu, Z., Gan, W., Zhan, X., Li, J., and Qiang, T. (2016). "Negative oxygen ions production superamphiphobic and antibacterial TiO_2/Cu_2O composite film anchored on wooden substrates," *Sci. Rep.-UK* 6. DOI: 10.1038/srep26055

Georgakilas, V., Otyepka, M., Bourlinos, A. B., Chandra, V., Kim, N., Kemp, K. C., Hobza, P., Zboril, R., and Kim, K. S. (2012). "Functionalization of graphene: Covalent and non-covalent approaches, derivatives and applications," *Chem. Rev.* 112(11), 6156-6214. DOI: 10.1021/cr3000412

GB/T 1933-2009 (2009). "Method for determination of the density of wood," Chinese National Standardization Management Committee, Beijing, China.

GB/T 1935-2009 (2009). "Method of testing in compressive strength parallel to grain of wood," Chinese National Standardization Management Committee, Beijing, China.

GB/T 1936.1-2009 (2009). "Method of testing in bending strength of wood," Chinese National Standardization Management Committee, Beijing, China.

Gooch, J. W. (2011). *Encyclopedic Dictionary of Polymers,* J. W. Gooch (ed), Springer, New York. DOI: 10.1007/978-1-4419-6247-8_865

Gwon, J. G., Lee, S. Y., Doh, G. H., and Kim, J. H. (2010). "Characterization of chemically modified wood fibers using FTIR spectroscopy for biocomposites," *J. Appl. Polym. Sci.* 116(6), 3212-3219. DOI: 10.1002/app.31746

Horikawa, Y., Itoh, T., and Sugiyama, J. (2006). "Preferential uniplanar orientation of cellulose microfibrils reinvestigated by the FTIR technique," *Cellulose* 13(3), 309-316. DOI: 10.1007/s10570-005-9037-9

Hou, H., Shang, M., Wang, L., Li, W., Tang, B., and Yang, W. (2015). "Efficient photocatalytic activities of TiO_2 hollow fibers with mixed phases and mesoporous walls," *Sci. Rep.-UK* 5. DOI: 10.1038/srep15228

Jiang, G., Lin, Z., Chen, C., Zhu, L., Chang, Q., Wang, N., Wei, W., and Tang, H. (2011). "TiO_2 nanoparticles assembled on graphene oxide nanosheets with high photocatalytic activity for removal of pollutants," *Carbon* 49(8), 2693-2701. DOI: 10.1016/j.carbon.2011.02.059

Khalid, N., Ahmed, E., Hong, Z., Sana, L., and Ahmed, M. (2013). "Enhanced photocatalytic activity of graphene-TiO_2 composite under visible light irradiation," *Curr. Appl. Phys.* 13(4), 659-633.

Liu, X., Zhang, H., Ma, Y., Wu, X., Meng, L., Guo, Y., and Liu, Y. (2013). "Graphene coated silica as a highly efficient sorbent for residual organophosphorus pesticides in water," *J. Mater. Chem. A* 1(5), 1875-1884. DOI: 10.1039/c2ta00173j

Posa, V. R., Annavaram, V., Koduru, J. R., Bobbala, P., and Somala, A. R. (2016). "Preparation of graphene-TiO_2 nanocomposite and photocatalytic degradation of Rhodamine-B under solar light irradiation," *J. Exp. Nanosci.* 11(9), 722-736. DOI: 10.1080/17458080.2016.1144937

Qiu, B., Zhou, Y., Ma, Y., Yang, X., Sheng, W., Xing, M., and Zhang, J. (2015). "Facile synthesis of the Ti_3^+ self-doped TiO_2-graphene nanosheet composites with enhanced photocatalysis," *Sci. Rep.-UK* 5. DOI: 10.1038/srep08591

Rahman, M. R., Hamdan, A. S., and Islam, M. S. (2010). "Mechanical and biological performance of sodium metaperiodate-impregnated plasticized wood (PW)," *BioResources* 5(2), 1022-1035.

Shao, X., Lu, W., Zhang, R., and Pan, F. (2013). "Enhanced photocatalytic activity of TiO_2-C hybrid aerogels for methylene blue degradation," *Sci. Rep.-UK* 3. DOI: 10.1038/srep03018

Shi, E., Xia, C., Wang, B., and Zhong, W. (1996). "Development and application of hydrothermal method," *J. Inorg. Mater.* 11(2), 193-206.

Sirota, T. V., Novoselov, V. I., Safronova, V. G., Yanin, V. A., Tsvetkov, V. D., Amelina, S., Lushnikova, A. L., Maltseva, V. N., Tikhonov, V. P., and Kondrashova,

M. N. (2006). "The effect of inhaled air ions generated by technical ionizers and a bioionizer on rat trachea mucosa and the phagocytic activity of blood cells," *IEEE T. Plasma Sci.* 34(4), 1351-1358. DOI: 10.1109/TPS.2006.877647

Sirota, T. V., Safronova, V. G., Amelina, A. G., Mal'tseva, V. N., Avkhacheva, N. V., Sofin, A. D., Yanin, V. A., Mubarakshina, E. K., Romanova, L. K., and Novoselov, V. I. (2008). "The effect of negative air ions on the respiratory organs and blood," *Biophysics* 53(5), 457-462. DOI: 10.1134/S0006350908050242

Tan, J. C., and Cheetham, A. K. (2011). "Mechanical properties of hybrid inorganic–organic framework materials: Establishing fundamental structure–property relationships," *Chem. Soc. Rev.* 40(2), 1059-80. DOI: 10.1039/C0CS00163E

Tom, G., Poole, M. F., Galla, J., and Berrier, J. (1981). "The influence of negative air ions on human performance and mood," *Hum. Factors* 23(5), 633-636. DOI: 10.1177/001872088102300513

Walton, S. G., Leonhardt, D., Fernsler, R. F., and Meger, R. A. (2003). "On the extraction of positive and negative ions from electron-beam-generated plasmas," *Appl. Phys. Lett*. 83(4), 626-628. DOI: 10.1063/1.1595155

Wang, J., Chen, Z., and Chen, B. (2014). "Adsorption of polycyclic aromatic hydrocarbons by graphene and graphene oxide nanosheets," *Environ. Sci. Technol.* 48(9), 4817-4825. DOI: 10.1021/es405227u

Yang, K., Chen, B., and Zhu, L. (2015). "Graphene-coated materials using silica particles as a framework for highly efficient removal of aromatic pollutants in water," *Sci. Rep.-UK* 5. DOI: 10.1038/srep11641

Yang, K., Wang, J., and Chen, B. (2014). "Facile fabrication of stable monolayer and few-layer graphene nanosheets as superior sorbents for persistent aromatic pollutant management in water," *J. Mater. Chem. A* 2(43), 18219-18224. DOI: 10.1039/c4ta04300f

Yao, Q., Wang, C., Fan, B., Wang, H., Sun, Q., Jin, C., and Zhang, H. (2016). "One-step solvothermal deposition of ZnO nanorod arrays on a wood surface for robust superamphiphobic performance and superior ultraviolet resistance," *Sci. Rep.-UK* 6. DOI: 10.1038/srep35505

Zeng, J., Liu, S., Cai, J., and Zhang, L. (2010). "TiO_2 immobilized in cellulose matrix for photocatalytic degradation of phenol under weak UV light irradiation," *J. Phys. Chem. C* 114(17), 7806-7811. DOI: 10.1021/jp1005617

Zhang, X., Hu, C., Bai, H., Yan, Y., Li, J., Yang, H., Lu, X., and Xi, G. (2013). "Construction of self-supported three-dimensional TiO_2 sheeted networks with enhanced photocatalytic activity," *Sci. Rep.* 3, 3563. DOI: 10.1038/srep03563

Zhong, L., Xiao, D., and Wu, C. (1998). "Aeroanion researches in evaluation of forest recreation resources," *Chin. J. Ecol.* 17(6), 56-60.

Zhou, K., Zhu, Y., Yang, X., Jiang, X., and Li, C. (2011). "Preparation of graphene–TiO_2 composites with enhanced photocatalytic activity," *New J. Chem.* 35(2), 353-359. DOI: 10.1039/c0nj00623h

Zou, H., Wu, S., and Shen, J. (2008). "Polymer/silica nanocomposites: Preparation, characterization, properties, and applications," *Chem. Rev.* 108(9), 3893-3957. DOI: 10.1021/cr068035q.

Article submitted: September 5, 2018; Peer review completed: December 15, 2018; Revised version received and accepted: December 20, 2018; Published: January 17, 2019.
DOI: 10.15376/biores.14.1.1781-1793